Applied Clay Science 71 (2013) 42–48

Contents lists available at SciVerse ScienceDirect

Applied Clay Science

journal homepage: www.elsevier.com/locate/clay

Research paper

Lignosulfonate interleaved layered double hydroxide: A novel green organoclay for bio-related polymer

Mohammed Hennous [a], Zoubir Derriche [a], Edwige Privas [b], Patrick Navard [b,1], Vincent Verney [c], Fabrice Leroux [c,*]

[a] Laboratoire de physico chimie des Matériaux, Catalyse et Environnement, Université des Sciences et de la Technologie d'Oran — BP 1505 El M'naouer, Oran 31000, Algeria
[b] Mines Paris Tech, CEMEF — Centre de Mise en Forme des Matériaux, CNRS UMR 7635, BP 207, 1 rue Claude Daunesse, 06904 Sophia Antipolis Cedex, France
[c] Institut de Chimie de Clermont-Ferrand, ICCF, CNRS, UMR 6096, Université Blaise Pascal, F-63177 Aubière, France

ARTICLE INFO

Article history:
Received 16 April 2012
Received in revised form 15 October 2012
Accepted 16 October 2012
Available online 8 December 2012

Keywords:
Layered double hydroxides
Hydrotalcite-like materials
Organoclays
Polyester bio-nanocomposites
Relation dispersion state and rheological properties

ABSTRACT

New organic inorganic layered double hydroxide (LDH) organoclays are assembled through coprecipitation with lignosulfonate (LS) interleaved inorganic host structure sheets. The biopolymer is found to accommodate the interlayer space adopting a bilayer molecular arrangement resulting in a basal spacing of 2.54 nm. However the crystallinity of the resulting bio-organoclay is weak, probably due to the difficulty of the inorganic sheets to be built on amorphous polymer chain, the latter inducing low structural ordering. An organoclay of composition Zn_2Al/LS is subsequently used as filler in three bio-related polyesters, poly(lactic) acid (PLA), poly(butylene) succinate (PBS) and poly(butylene adipate-co-terephthalate) (PBAT). Melt polymer extrusion using 5 wt.% organoclay loading yields polyester nanocomposite with a nanocomposite structure largely intercalated for both PLA and PBS (Δd (expansion) > 6 nm) while a non miscible structure is obtained for PBAT. The incorporation of hydrophilic Zn_2Al/LS platelets decreases the water/polymer contact angle of about 10° for the LDH/LS PBAT composite only. A strong increase of the complex viscosity $|\eta^*|$ is observed for both nanocomposites Zn_2Al/LS PLA and PBS compared to the polyester itself. This is explained on the basis of a chain extender behavior of the intercalated Zn_2Al/LS platelets towards polymer chains as evidenced on the Cole Cole representation showing an increase of the real viscosity in the low-ω region. In opposition a strong decrease in $|\eta^*|$ is observed for PBAT, underlining a plasticizing effect of the organoclay filler. Comparatively, the thermal stability of PLA is slightly enhanced with an increase of $T_{0.5}$ value while PBS and PBAT bio-nanocomposites degrade at slightly lower temperature.

1. Introduction

The ever-growing environmental concern framed into an ever-stronger regulation is currently stimulating intense research all over the world to replace fossil energy-based polymer. Indeed there is a lot at stake facing this environmental concern, and the problem may be partially solved by recycling or using alternative degradable materials. Taking into account the requirement for a sustainable development such alternative should also be of interest in terms of performance. For instance biodegradable polymers are interesting not only in disposable packaging but also for different applications such as bone substitute, scaffold and drug carrier for controlled release.

To overcome such issues, biodegradable nanocomposite are more and more considered as the "next generation" for the future (Domb et al., 1997; Pandey et al., 2005; Tsuji and Horikawa, 2007), this with the possible combination with environmental-friendly organoclay as filler. Indeed biopolymers or bio-degradable polymers candidate to replace polyolefin suffer generally of poor physical properties and consequently their applications are up to now limited while the incorporation of organoclays may provide mechanical reinforcement, barrier effect as well as fire retardancy properties, thus fulfilling the specific requirements for their potential use.

Organo-modified clays are extensively studied for their possibilities to enhance polymer properties (Paul et al., 2003), and among them layered double hydroxide (LDH) materials present a certain advantage (Leroux, 2006). Indeed different authors have pointed out the versatility of LDH materials for fabricating nanocomposites (Ding et al., 2006; Evans and Duan, 2006), as the lamellar nature of LDHs permits host guest chemistry and intercalation reactions, which invoke considerable attention from material designers (Leroux et al., 2010). Layered Double Hydroxide also called "anionic" clay in comparison to smectite-type materials is formed from edge-sharing octahedral, and its structure is described from the substitution divalent by trivalent cations in the brucite $Mg(OH)_2$. The resulting cation composition $M^{II}_{1-x}M^{III}_x(OH)_2$ with x being the relative substitution rate generally ranging as $0.20 < x < 0.33$, endows a positive charge to the sheet counterbalanced

* Corresponding author. Tel.: +33 473407036.
E-mail address: Fabrice.Leroux@univ-bpclermont.fr (F. Leroux).
[1] Member of the European Polysaccharide Network of Excellence, www.epnoe.eu.

0169-1317/$ – see front matter © 2012 Elsevier B.V. All rights reserved.
http://dx.doi.org/10.1016/j.clay.2012.10.011

by the presence of anion in the interlayer space. The surface covered by hydroxyl groups and the great versatility in the cation and anion exchange with suitable organic molecule are highly suitable in flame retardancy application (Evans and Duan, 2006) and the presence of hydroxyl groups renders the particles hydrophilic. Lateral dimensions through the LDH plate ranging from 100 nm to 1–2 μm, and a width of 1 to 3 nm for the organo-modified hybrid platelets give rise to aspect ratio between limits of 100 to 2000, which are potentially interesting for the increase of turtuosity (permeation) and for the mechanical reinforcement (Utracki et al., 2007).

Poly(esters) are among the most promising materials for the production of high-performance and environmental-friendly biodegradable polymer and among them, polylactic acid (PLA), poly(butylene) succinate (PBS) (Lim et al., 2011a,b), and polybutylene adipate terephthalate (PBAT) (Chen et al., 2011; Mohanty and Nayak, 2010; Raquez et al., 2011; Siegenthales et al., 2012; Yang and Qiu, 2011) and the corresponding mixings PLA/PBAT (Kumar et al., 2010; Li et al., 2011) PBS/PBAT (Ibrahim et al., 2010) have recently received a lot of attention.

PLA and PBS are linear aliphatic hydrophobic thermoplastic polyesters. PLA is produced from agricultural resources and by ring-opening polymerization of lactides, and can be easily degraded through hydrolytic process (Grizzi et al., 1995) or by enzymatic way (Edlund and Albertsson, 2001), and it suffers from heat distortion temperature, brittleness, low elongation and gas barrier properties. PBS is synthesized by polycondensation of 1,4-butanediol with succinic acid and presents some drawbacks such as low hydrolysis resistance, softness, tensile, gas-barrier properties and melt-viscosity not sufficient for processing for a practical end-use application (Zhou et al., 2010). PBAT, a biodegradable aliphatic-aromatic polyester, named as Ecoflex® (Siegenthales et al., 2012) combines biodegradability known from its aliphatic moieties with mechanical properties from its aromatic moieties.

The dispersion of organo-modified LDH into biodegradable polymer was scarcely reported, including poly(caprolactone) (PCL) (Mangiacapra et al., 2007; Sorrentino et al., 2005), but recent gain in interest is reported for PLA (Chiang et al., 2011; Ha and Xanthos, 2010; Katiyar et al., 2011; Mahboobeh et al., 2010; Wang et al., 2010) and specifically for assessment of the suitability of the polymer films for use as food contact materials (Schmidt et al., 2011) as well as drug delivery system such as LDH framework dispersed into PLA to vehicle ibuprofen (Dagnon et al., 2009) or alendronate (Chakraborti et al., 2011). This is also available for PBS with functionalized filler for ecological photoactive surface (Kafunkova et al., 2010). Comparatively some studies concern the dispersion of commercially-available organically modified montmorillonite with a particular interest for poly(butylenes succinate-co-adipate) (Dean et al., 2009; Ray and Bousmina, 2006).

Having in mind that the filler in its entire composition should be "green", it implies that the organo modifying molecule should be bio-eminent or at least environmentally benign, while LDH platelets (of selected composition) are considered as biocompatible (Bugatti et al., 2011; Choy et al., 2007; Costantino et al., 2008; Oh et al., 2009) and as possible food contact materials (Schmidt et al., 2011). Moreover it is well known that the inorganic LDH host structure presents the ability to accommodate cumbersome macromolecule, such as DNA (Choy et al., 1999), alginate (Leroux et al., 2004) and other polysaccharides (Darder et al., 2005). Lignosulfonate (LS), a water-soluble biopolymer obtained from wood industry is here selected. However the fact that lignosulfonate is known as efficient plasticizers in making concrete (Collins et al., 2012), debundling of single-walled carbon nanotubes (Liu et al., 2007), destructuring of inter- and intramolecular interactions within bionanocomposites (Oliviero et al., 2011) as well as presenting a strong hydrophilic character makes it at the first glance not really promising to organo-modify LDH platelets. In contrast the biodegradability of PBAT bio-nanocomposite showed an increase in the rate of biodegradability using Na-montmorillonite due to its hydrophilic nature (Mohanty and Nayak, 2010). Therefore it is here crucial to know whether the dispersion of such appealing bio-concerned LDH organoclay is efficient as filler for polymer.

LDH/LS assembly first characterized by a combination of techniques (XRD, FTIR, and solid state ^{13}C CPMAS NMR) is subsequently dispersed through polymer melt extrusion into PLA, PBS and PBAT, respectively. The polymer dispersion is scrutinized by low angle XRD, and the microstructure is evaluated by rheology and addressed as a function of the dispersion of the bio-hybrid LDH filler. A series of biodegradable polymer nanocomposites, hereafter noted as PLA:LDH/LS, PBS:LDH/LS and PBAT:LDH/LS, is successively characterized by X-ray diffraction, and rheology to undecipher the attritive or plastizicing role of the organoclay. Finally the thermal properties of the bionanocomposite are also studied.

2. Experimental section

2.1. Materials

$ZnCl_2$, $CoCl_2\ 6H_2O$, $MgCl_2\ 6H_2O$, $Al(NO_3)_3 \cdot 9H_2O$ (Acros, 99%), NaOH (Acros, 97%) and water-soluble anionic polyelectrolyte lignosulfonate sodium polymer (Aldrich, $C_{10}H_{12}O_5SNa$, $M_n = 7000\ g \cdot mol^{-1}$, $M_w = 52{,}000\ g \cdot mol^{-1}$, CAS # 8061-51-6) were used as received. Poly(lactic acid) (CAS#33135-50-1) (PLA, $-(-CH(CH_3)\text{-}CO\text{-}O\text{-})_n-$) density of 1.25 g/cm^3, glass transition temperature (T_g) of 60.7 °C and melting point (T_m) of 165.1 °C was supplied by Natureworks (4042-D, USA). PBS (CAS#25777-14-4) EnPol G-4560 (MI = 1.5 g/10 min, Tm = 115 °C) was provided by Ire Chemicals Co. Korea. Statistical copolyester PBAT (Ecoflex) was supplied by BASF Company.

2.2. Organo-modification of LDH

The cation LDH composition was Zn_2Al, and the preparation of the hydrotalcite-like hybrid materials was performed using the so-called coprecipitation method. Experimentally, solution of lignosulfonate ($2 \cdot 10^{-2}$ M) was prepared, and 250 ml solution of the salts (Zn; $2 \cdot 10^{-2}$ M and Al; $1 \cdot 10^{-2}$ M) was added dropwise to the previous solution. During the addition, the reaction was kept under nitrogen atmosphere in order to avoid contamination by carbonate and the pH was kept constant at pH = 9.5 ± 0.1 with the addition of NaOH. The slurry was aged in the mother liquid and separated by centrifugation. The resulting powders hereafter named as Zn_2Al/LS was washed several times with distilled water and finally dried at room temperature. Two other LDH compositions were synthesized in similar condition using Mg:Al (2:1) and Co:Al (2:1) and pH coprecipitation value of 10 ± 0.1 and 8 ± 0.1, respectively.

2.3. Preparation of the biodegradable polymer nanocomposite

Prior to their preparation, the three polyesters were dried at 40 °C for 48 h in air oven, while Zn_2Al/LS organoclay was dried at 100 °C for 2 h. The three thermoplastic polyesters were melt-processed on a standard micro-extruder equipment at 170 °C (5′), 120 °C (5′) and 140 °C (10′) in a twin screw extruder (rotation 100 rpm) for PLA, PBS and PBAT, respectively. Organoclay loading was of 5 wt.%. For further analyses, polymer films were prepared by hot pressing.

2.4. Characterization

Elemental analysis (S, Al and Zn) was performed at the Vernaison Analysis Center of CNRS using inductive conduction plasma coupled to atomic emission spectroscopy (ICP/AES). The chemical compositions were reported from elemental analyses, Zn, Al, S at.%.

XRD analyses of the hybrid LDH and polymer nanocomposites were performed on a Siemens D501 diffractometer using Cu K_α source (30 mA, 35 kV); data were collected in a step scan mode between 2.0 and 70.0°(2θ) and with a step size of 0.03°(2θ) and a

counting time of 10 s/step. For the low-angle recording, measurements were performed closing the slits from 1 to 0.3° in the 2θ-range 1 or 0.7 to 10° with a step size 0.005°, and step counting time of 20 s.

Rheological measurements were carried out on a rheometer Rheometric Scientific equipped with a parallel plate geometry using 8 mm diameter plates and using a gap of 1 mm. The dynamic strain sweep measurements were carried out to determine the linear viscoelastic region, and a temperature of 170, 120 and 140 °C was applied on PLA, PBS and PBAT and LDH nanocomposite derivatives, respectively.

Thermogravimetric analysis (TGA) was performed under air using Setaram equipment. Heating slope was of 5 °C/min, from 15° to 1100 °C.

Static water contact angles were measured using a sessile drop at three different points of each film sample using a optical contact angle KSVs CAM 101 (Helsinki, Finland) at ambient temperature. The volume of water droplets used was 10 μl.

3. Results and discussion

3.1. Organo-modified LDH

3.1.1. XRD results of hybrid LDHs

As-prepared Zn_2Al/LS hybrid material presents a poor crystallinity, however the few observed reflections are consistent with the formation of a LDH phase as shown in Fig. 1(a). The reflections at 30° and 60° are characteristic of LDH structure and associated to (101) and (110) diffraction reflections respectively, in the rhombohedral symmetry adopting the space group R-3 m as usually used to describe LDH structure. The reflection at low 2θ values is associated to the basal spacing, and the recording in the lower 2θ domain permits to locate more precisely its value of 2.54 nm. The latter suggests the incorporation of the biopolymer presumably in a double layer accommodation taking into account the polymer dimension.

The width of the X-ray reflection rather large as well as the quasi absence of harmonic reflection is interpreted by an ill-defined stacking of the hybrid LDH material. The low crystallinity can be here interpreted by the amorphous nature of the biopolymer (*i.e.* absence of long range chain order) thus not assisting the coprecipitation from a structural point of view, and therefore yielding to ill-defined hybrid LDH assembly. This is reminiscent of other hybrid LDH structure interleaved with other related biopolymer such as alginate (Leroux et al., 2004) or carrageen (Darder et al., 2005).

XRD patterns for Mg_2Al- and Co_2Al/LS (Fig. 1(b and c)) present similar features associated to the incorporation of lignosulfonate within the interlayer domain but yielding to even more pronounced ill-defined hybrid assemblies. The crystallinity is ranged as followed: Co_2Al/LS < Mg_2Al/LS < Zn_2Al/LS. Spectroscopic analyses (FTIR and solid state NMR ^{13}C CP MAS) confirm the presence of lignosulfonate in the hybrid material (supporting information).

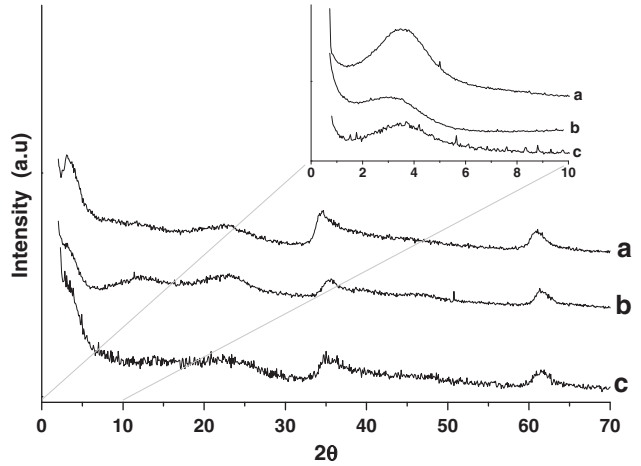

Fig. 1. XRD of hybrid LDH phases: a) Zn_2Al/LS, b) Mg_2Al/LS and c) Co_2Al/LS.

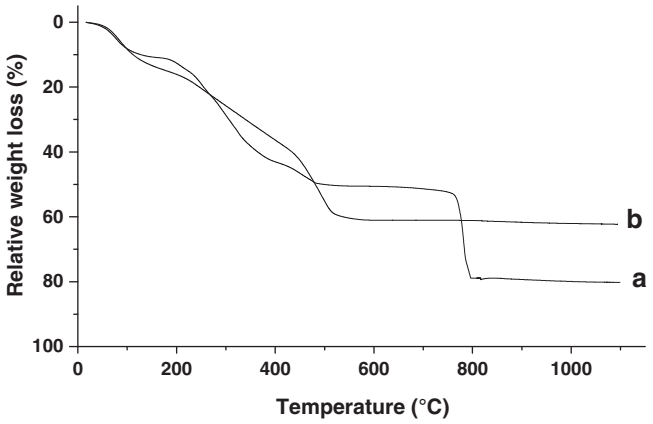

Fig. 2. TGA analysis for a) sodium lignosulfonate (Na–LS), b) Zn_2Al/LS.

3.1.2. TG analysis

Lignosulfonate decomposes in several steps (Fig. 2(a)) with a final end-product at 1100 °C identified as Na_2SO_4. The final weight loss of 80% suggests a hydration rate of 4.9 water molecule per formula weight $C_{10}H_{12}O_{10}SNa$. If one surmises that such amount corresponds to physi-sorbed water, its departure corresponding to 24.8 wt.% is expected at temperature lower than 200 °C. This is in discrepancy with the data, showing that the hydration rate of the biopolymer is overestimated, probably due to the presence of lignine not sulfonated.

In the following it is interesting to note that non sulfonated polymer should not be contributing to the organoclay formation, the coprecipitation process acting as selective sieves which impede the neutral polymer chain to interact with the inorganic sheets. The organoclay Zn_2Al/LS decomposes in several thermal events differently from the biopolymer itself. TG analysis (Fig. 2(b)) in combination with XRD phase identification results in the formation at high temperature of ZnO and the spinel phase $ZnAl_2O_4$. Evidently by-product formation is dependent of the platelet chemical composition (Mg: Al, and Co:Al). The final weight loss at 1100 °C of 60% suggests a hydration rate of 1.7 water molecule per formula weight $Zn_2Al(OH)_6$, thus yielding to a molecular weight of Mw = 534.4 $g \cdot mol^{-1}$ adopting Zn_2Al/LS as $Zn_2Al(OH)_6(C_{10}H_{12}O_5S)_{1.00}$. 1.7 H_2O. This agrees well the elemental analysis Zn: 24.5% (exp: 24.47%), Al: 4.98% (exp: 5.05%) and S: 6.05% (exp: 6.00%).

3.2. LDH/LS: polyester composites

3.2.1. XRD analysis

All three polymers are semi-crystalline polyesters. Concerning PLA, an ill-defined reflection is observed at 2θ = 16.5° (Fig. 3), corresponding

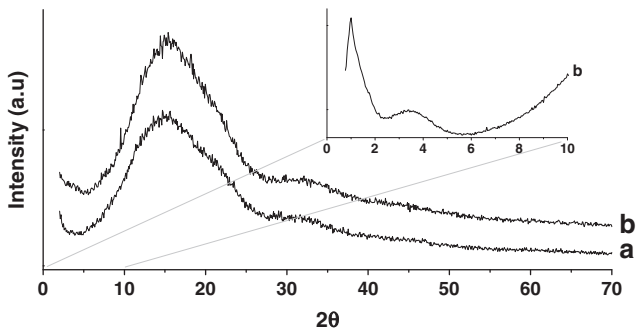

Fig. 3. X-Ray diffractograms of a) PLA and PLA–Zn_2Al/LS.

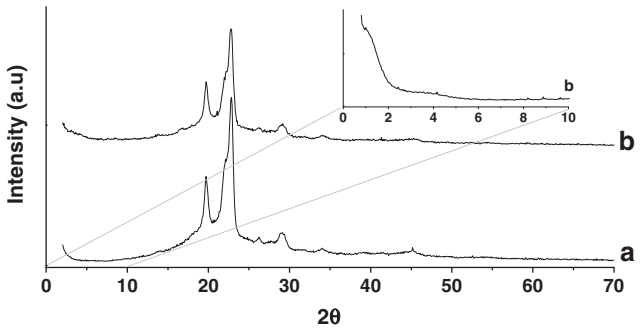

Fig. 4. X-Ray diffractograms of a) PBS and PBS–Zn_2Al/LS.

to a spacing of 0.534 nm (Krikorian and Pochan, 2003), the other usual spacings are not observed because of the presence of a large hump coming from a large amorphous contribution within PLA. As shown in Fig. 4, the XRD pattern of PBS is in agreement with the literature (Ray et al., 2003). Indeed, X-ray pattern exhibits reflections at $2\theta = 19.7°$, 22.1°, and 22.8°, which are assigned to (020), (021) and (110) planes of α-form PBS crystal, respectively. PBAT is a copolyester with a statistical description poly(butylene adipate-co butylene terephthalate), the diffraction pattern is in agreement with the literature (Kuwabara et al., 2002) (Fig. 5).

Comparing the polyester Zn_2Al/LS polymer nanocomposite, the associated XRD exhibits the diffraction lines characteristic of the polymer signature (Fig. 5), that is to mention with no modification neither in line-width nor in position of the diffraction lines, thus indicating that the structure (*i.e.* polymorphism) and the corresponding crystallized domains of the polyesters are not perturbed by the presence of hybrid LDH tactoids.

Concerning the layered structure of the organoclay, the diffraction lines characteristic of the in-plane order are barely observed. This can be explained by the low amount of diffracting platelets (5 wt.%) as well as a cumulative effect of an initial ill-defined assembly and the deleterious effect of extrusion on the organoclay crystallinity. Nevertheless an intercalated PLA nanocomposite structure is observed at low $2\theta = 1.0°$ (8.8_3 nm) (Fig. 3(b)), it corresponds to an increase of $\Delta d = 6.2_9$ nm from the initial Zn_2Al/LS basal spacing. Such large increase in the organoclay basal spacing has to be interpreted by PLA chains diffusing between the organo-modified LDH platelets. Other PLA intercalated structures are reported for LDH organo-modified by laurate, even if agglomeration is also observed (Katiyar et al., 2011). Similarly a shoulder is observed in the low-θ values for PBS nanocomposite (Fig. 4(b)). Its location at $2\theta \approx 1°$ suggests as well a PBS nanocomposite structure strongly intercalated. Such large intercalated polymer nanocomposite structure has been recently reported for other LDH filler dispersed into polyurethane (Swanson et al., 2012). The possibility of polyester chains to diffuse within the interlayer space of LDH framework agrees

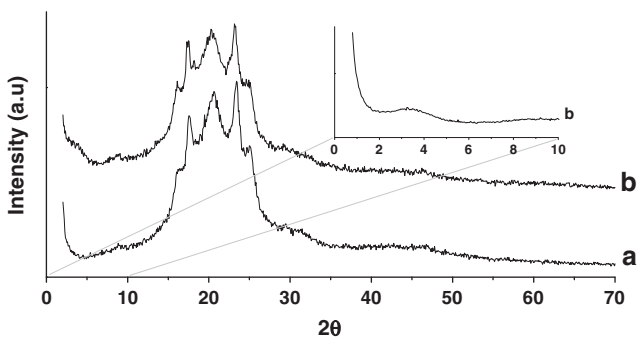

Fig. 5. X-ray diffractograms of a) PBAT and PBAT–Zn_2Al/LS.

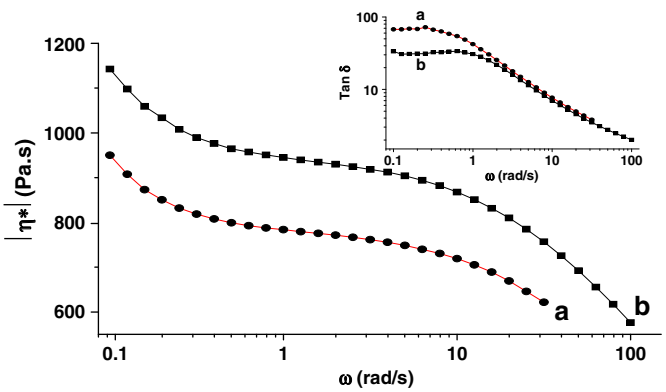

Fig. 6. Complex viscosity $|\eta^*|$ *vs.* ω for a) PLA and PLA–Zn_2Al/LS. In the inset is a representation of the corresponding tan δ *vs.* ω.

well with LS accommodated as a double-layer rather than as a single layer that would have impede any intercalation process within the organoclay. For PBAT and Zn_2Al/LS mixture, a small reflection is observed located at the same position than that of Zn_2Al/LS ($2\theta \approx 3.5°$). This indicates in that case the presence of non-miscible structure between the polyester and the organoclay. This difference in dispersion may be related to the difference in the polymer backbone, with aliphatic linear chains apparently easier for them to diffuse in between LDH sheets than a statistical copolymer bearing terephthalate function. It is also interesting to mention that when Cloisite was dispersed into a PLA/PBAT blend (Li et al., 2011), the nanoclay platelets were found to locate at the interface improving the adhesion between polymers but not dispersing in one of them.

3.2.2. Rheology

To further discriminate between the obtained polyester composite structures, the subsequent effect on the polymer microstructure is scrutinized by rheological analysis. The variation of the complex viscosity $|\eta^*|$ *vs.* ω is shown in Figs. 6 to 8. An increase is observed for both PLA and PBS composites indicating that the molecular weight of the polymer has increased. This is associated to a lowering of the damping coefficient tan δ ($= G''/G'$) in the low-ω range, $\omega < 0.5$ rad/s (inset of Figs. 6 and 7).

In the related terminal zone, such change is usually related to some restricted segmental motions at the interface between filler and polymer chain. Such flow restriction of the polyester chain is caused usually by an increase in the chain dimension until it reaches a transition from liquid (Newtonian polymer) to gel-like structure. However the latter phenomenon is already observed on PLA and PBS free of charge with the shear-thinning factor n visible at low ω, $|\eta^*|$ tends to ω^n. The slope that is related to the power-law tendency for $|\eta^*|$ is not modified with the incorporation of Zn_2Al/platelets, thus

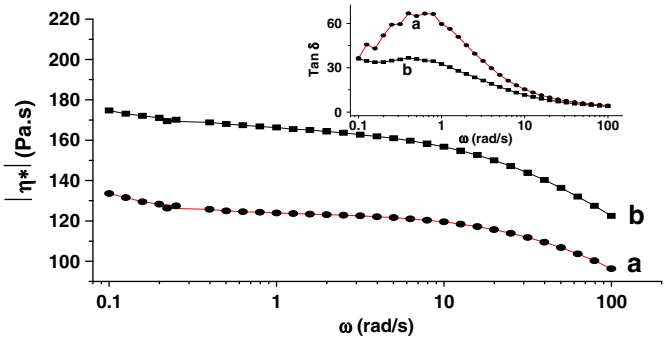

Fig. 7. Complex viscosity $|\eta^*|$ *vs.* ω for a) PBS and PBS–Zn_2Al/LS. In the inset is a representation of the corresponding tan δ *vs.* ω.

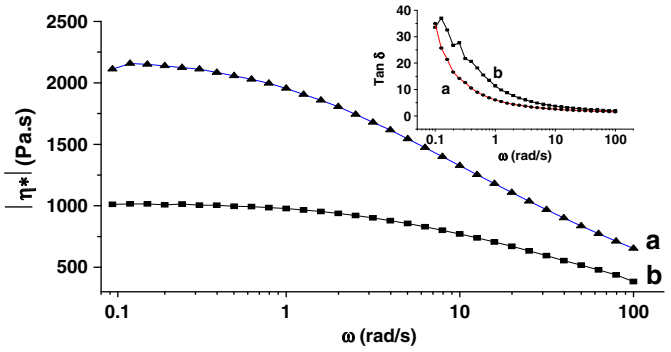

Fig. 8. Complex viscosity $|\eta^*|$ *vs.* ω for a) PBAT and PBAT-Zn_2Al/LS. In the inset is a representation of the corresponding tan δ *vs.* ω.

showing that the decrease in relaxation is not due to a network formation but rather to an extension of the polymer chains only. This is evidenced by plotting the rheological data in Cole–Cole representation, η''–$\eta'(\omega)$ (Figs. 9, 10 and 11). A depressed semi-circle is observed with a straight line, the former corresponds to the Newtonian behavior while the latter to the presence of a gel-like polyester structure with no apparent finite molecular weight. There is no change in the latter structure. However the semi-circle is strongly modified for the three polyester composites.

The convex downward semi-circle profile at the intercept η" which tends to 0 and corresponds to the Newtonian zero-shear viscosity η'_0 at $\omega = 0$, is shifted to a higher value for PLA and PBS (Figs. 9 and 10) and to a lower value for PBAT (Fig. 11). From DSC and FTIR spectral analyses, intermolecular interaction was surmised for blends of PLA and lignin (Li et al., 2003), while it was found that calcium lignosulfonate improves the crystalline properties of PBS (Lin et al., 2011). However these observations were performed on lignin or LS content used as much as 20 wt.% to be compared to 2.5 wt.% used here when loading with 5 wt.% of Zn_2Al/LS organoclay.

Since the value of η'_0 is proportional to M_w according to a power-law $\eta'_0 = K.M_w^{3.4}$, it can be understood as a chain extension for PLA and PBS composite and to a chain reduction for PBAT. Contrary to PLA and PBS, the latter behavior is explained by a plasticizing effect of the organoclay for PBAT chains having as a consequence a reduction of η'_0, a decrease in the complex viscosity and inversely an increase of tan δ at low ω (Figs. 8 and 11). Even intercalated, laurate organo-modified LDH was found to reduce the PLA molecular weight (Katiyar et al., 2011).

This can be easily related to both intercalated PLA and PBS nanocomposite structures with an interface between the organoclay and aliphatic polyester chains strongly developed. One cannot discard

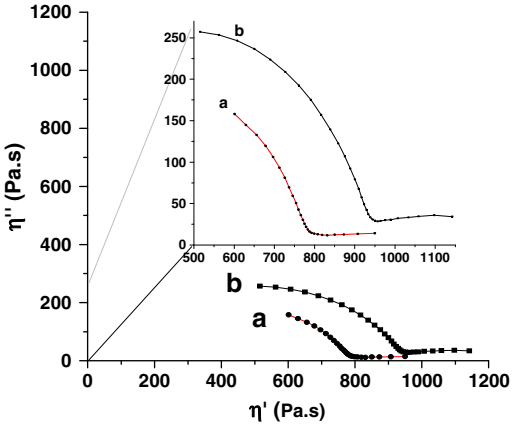

Fig. 9. Cole Cole representation η'' *vs.* η' (ω) for a) PLA and PLA–Zn_2Al/LS. An enlarged domain is displayed in inset to visualize η'_0.

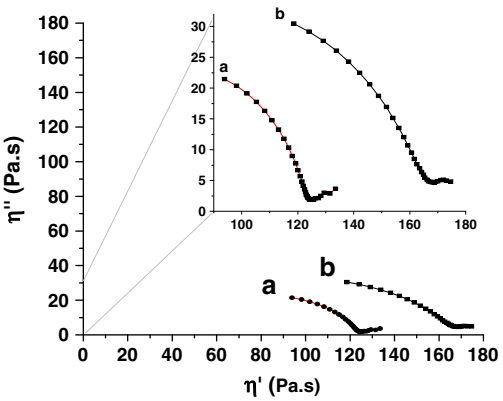

Fig. 10. Cole Cole representation η'' *vs.* η' (ω) for a) PBS and PBS–Zn_2Al/LS. An enlarged domain is displayed in inset to visualize η'_0.

some attritive reactions between –(CH_2OH) LS functions and the polyester carbonyl function. In contrast such phenomenon is not available for PBAT, probably due to the presence of the cycle in the vicinity of the carbonyl, but the change in the rheological behavior shows that even a non miscible polymer structure can strongly affect the polymer as previously demonstrated in the case of LDH polystyrene composites (Illaik et al., 2008). One should mention that the use of larger loading (10 wt.%) is deleterious for all three polyesters (not shown).

3.2.3. Thermogravimetric analysis of organoclay polyester composites

The three polyesters start to decompose at temperature higher than 300 °C to reach a total combustion ending at 500 °C. A beneficial effect of Zn_2Al/LS on the weight loss curve with an onset of 8.55 °C obtained at half weight loss, $T_{0.5}$ can be observed. Such value is slightly decreased for PBS composite from 379.49 °C to 375.19 °C and much larger shifted to low temperature for PBAT than for PBAT composite from 363.91 °C to 388 °C.

3.2.4. Static water contact angle measurements

Water contact angle is measured by the well known sessile drop technique. The water contact angle is in the same range for the three polyesters (Fig. 12).

When Zn_2Al/LS organoclay is dispersed, the water contact angle remains identical for the intercalated polyester structure (PLA and PBS derivatives) while it drops for the non miscible PBAT composite of 10°. In the latter case, it underlines a greater surface hydrophilicity,

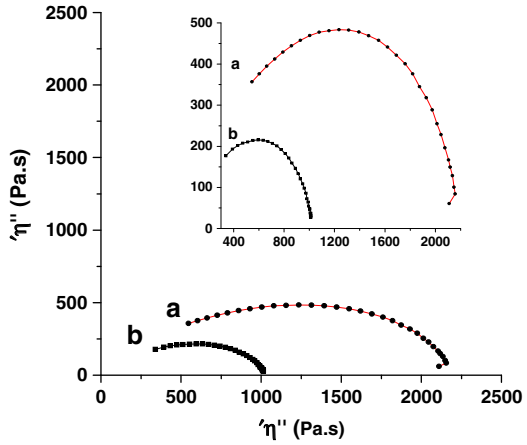

Fig. 11. Cole Cole representation η'' *vs.* η' (ω) for a) PBAT and PBAT–Zn_2Al/LS. An enlarged domain is displayed in inset to visualize η'_0.

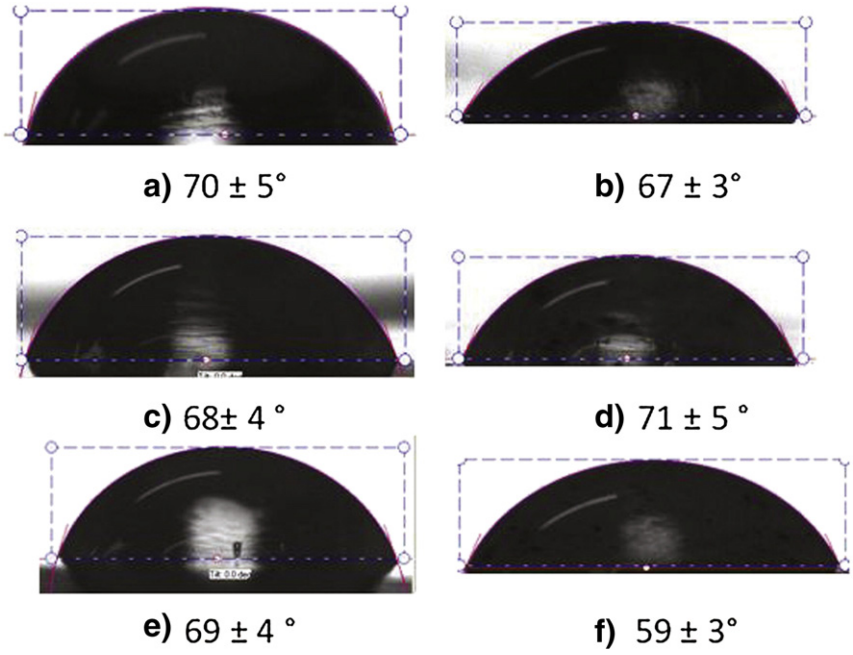

Fig. 12. Water contact angle for a) PLA, b) PLA–Zn_2Al/LS, c) PBS, d) PBS–Zn_2Al/LS, e) PBAT, and f) PBAT–Zn_2Al/LS.

this probably due to stacked Zn_2Al/LS hydrophilic assemblies segregated at the polymer surface.

4. Conclusions

Zn_2Al/LS is successfully synthesized by coprecipitation, giving rise to an ill-defined hybrid assembly. Counter intuitively the resulting hydrophilic organoclay is found to be of interest for polar polymer such as polyester. For PLA and PBS and using 5 wt.% loading, the measured rheological parameters increase in the whole domain of frequency. It is here interpreted as the organoclay acting as a chain-extender when its associated structure is intercalated by the polymer chain. The study underlines the strong attritive phenomenon responsible of such behavior and visible at low ω-region through an interface largely developed between the organoclay and the polyester chains. It is our belief that such bio-related organoclay will open new route for the design of nanocomposite polymer integrating eco- and bio-friendly requirements.

Acknowledgments

M.H. gratefully acknowledges a strategic bilateral cooperation program (Algerian France PROFAS) for funding as well as l'Ecole Nationale Supérieure de Chimie de Clermont-Ferrand (ENSCCF). The work of EP was performed in the frame of the Industrial Chair in Bioplastics supported by Arkema, l'Oréal, Nestlé, PSA Peugeot-Citroën and Schneider Electric.

Appendix A. Supplementary data

Supplementary data to this article can be found online at http://dx.doi.org/10.1016/j.clay.2012.10.011.

References

Bugatti, V., Gorrasi, G., Montanari, F., Nocchetti, M., Tammaro, L., Vittoria, V., 2011. Modified layered double hydroxides in polycaprolactone as a tunable delivery system: *in vitro* release of antimicrobial benzoate derivatives. Applied Clay Science 52, 34–40.

Chakraborti, M., Jackson, J.K., Plackett, D., Brunette, D.M., Burt, H.M., 2011. Drug intercalation in layered double hydroxide clay: application in the development of a nanocomposite film for guided tissue regeneration. International Journal of Pharmaceutics 416, 305–313.

Chen, J.-H., Chen, C.-C., Yang, M.-C., 2011. Characterization of nanocomposites of poly(butylene adipate-co-terephthalate) blending with organoclay. Journal of Polymer Research 18, 2151–2159.

Chiang, M.-F., Chu, M.-Z., Wu, T.-M., 2011. Effect of layered double hydroxides on the thermal degradation behavior of biodegradable poly(L-lactide) nanocomposites. Polymer Degradation and Stability 96, 60–66.

Choy, J.-H., Kwak, S.Y., Park, J.S., Jeong, Y.J., Portier, J., 1999. Intercalative nanohybrids of nucleoside monophosphates and DNA in layered metal hydroxide. Journal of the American Chemical Society 121, 1399–1400.

Choy, J.-H., Choi, S.-J., Oh, J.-M., Park, T., 2007. Clay minerals and layered double hydroxides for novel biological applications. Applied Clay Science 36, 122–132.

Collins, F., Lambert, J., Duan, W.H., 2012. The influences of admixtures on the dispersion, workability, and strength of carbon nanotube–OPC paste mixtures. Cement and Concrete Composites 34, 201–207.

Costantino, U., Ambrogi, V., Nocchetti, M., Perioli, L., 2008. Hydrotalcite-like compounds : versatile layered hosts of molecular anions with biological activity. Microporous and Mesoporous Materials 107, 149–160.

Dagnon, K.L., Ambadapadi, S., Shaito, A., Ogbomo, S.M., De Leon, V., Golden, T.D., Rahimi, M., Nguyen, K., Braterman, P.S., D'Souza, N.A., 2009. Poly(L-lactic acid) nanocomposites with layered double hydroxides functionalized with ibuprofen. Journal of Applied Polymer Science 113, 1905–1915.

Darder, M., Lopez-Blanco, M., Aranda, P., Leroux, F., Ruiz-Hitzky, E., 2005. Bio-nanocomposites based on layered double hydroxides. Chemistry of Materials 17, 1969–1977.

Dean, K.M., Pas, S.J., Yu, L., Ammala, A., Hill, A.J., Wu, D.Y., 2009. Formation of highly oriented biodegradable polybutylene succinate adipate nanocomposites: effects of cation structures on morphology, free volume, and properties. Journal of Applied Polymer Science 113, 3716–3724.

Ding, P., Chen, W., Qu, B., 2006. Recent progress in polymer/layered double hydroxide nanocomposites. Progress in Natural Science 16, 573–579.

Domb, A.J., Kost, J., Wiseman, D.M. (Eds.), 1997. Handbook of biodegradable polymers. Drug Targeting and Delivery, vol. 7. Harwood Academic Publishers, Amsterdam.

Edlund, U., Albertsson, A.-C., 2001. Degradable polymer microspheres for controlled drug delivery. Advances in Polymer Science 157, 67–112.

Evans, D.G., Duan, X., 2006. Preparation of layered double hydroxides and their applications as additives in polymers, as precursors to magnetic materials and in biology and medicine. Chemical Communications 485–496.

Grizzi, I., Garreau, H., Li, S., Vert, M., 1995. Hydrolytic degradation of devices based on poly(DL-lactic acid) size-dependence. Biomaterials 16, 305–311.

Ha, J.U., Xanthos, M., 2010. Novel modifiers for layered double hydroxides and their effects on the properties of polylactic acid composites. Applied Clay Science 47, 303–310.

Ibrahim, N.A., Chieng, B.W., Yunus, W.M.Z.W., 2010. Morphology, thermal and mechanical properties of biodegradable poly(butylene succinate)/poly(butylene adipate-co-terephthalate)/clay nanocomposites. Polymer — Plastics Technology and Engineering 49, 1571–1580.

Illaik, A., Taviot-Guého, C., Lavis, J., Commereuc, S., Verney, V., Leroux, F., 2008. Unusual polystyrene nanocomposite structure using emulsifier-modified layered double hydroxide as nanofiller. Chemistry of Materials 20, 4854–4860.
Kafunkova, E., Lang, K., Kubat, P., Klementova, M., Mosinger, J., Slouf, M., Troutier-Thuilliez, A.-L., Leroux, F., Verney, V., Taviot-Gueho, C., 2010. Porphyrin-LDH dispersed polymer composites as novel ecological photoactive surfaces. Journal of Materials Chemistry 20, 9423–9432.
Katiyar, V., Gerds, N., Koch, C.B., Risbo, J., Hansen, H.C.B., Plackett, D., 2011. Melt processing of poly(L-lactic acid) in the presence of organomodified anionic or cationic clays. Journal of Applied Polymer Science 122, 112–125.
Krikorian, V., Pochan, D.J., 2003. Poly(L-lactic acid)/layered silicate nanocomposite: fabrication, characterization, and properties. Chemistry of Materials 15, 4317–4324.
Kumar, M., Mohanty, S., Nayak, S.K., Parvaiz, M.R., 2010. Effect of glycidyl methacrylate (GMA) on the thermal, mechanical and morphological property of biodegradable PLA/PBAT blend and its. Bioresource Technology 101, 8406–8415.
Kuwabara, K., Gan, Z., Nakamura, T., Abe, H., Doi, Y., 2002. Crystalline/amorphous phase structure and molecular mobility of biodegradable poly(butylene adipate-co-butylene terephthalate) and related polyesters. Biomacromolecules 3, 390–396.
Leroux, F., 2006. Organo-modified anionic clays into polymer compared to smectite-type nanofiller: potential applications of the nanocomposites. Journal of Nanoscience and Nanotechnology 6, 303–315.
Leroux, F., Gachon, J., Besse, J.-P., 2004. Biopolymer immobilization during the crystalline growth of layered double hydroxide. Journal of Solid State Chemistry 177, 245–250.
Leroux, F., Illaik, A., Stimpfling, T., Troutier-Thuilliez, A.-L., Fleutot, S., Martinez, H., Cellier, J., Verney, V., 2010. Percolation network of organo-modified layered double platelets into polystyrene showing enhanced rheological and dielectric behaviors. Journal of Materials Chemistry 20, 9484–9494.
Li, J., He, Y., Inoue, Y., 2003. Thermal and mechanical properties of biodegradable blends of poly(L-lactic acid) and lignin. Polymer International 52, 949–955.
Li, K., Cui, Z., Sun, X., Turng, L.-S., Huang, H., 2011. Effects of nanoclay on the morphology and physical properties of solid and microcellular injection molded polyactide/poly(butylenes adipate-co-terephthalate) (PLA/PBAT) nanocomposites and blends. Journal of Biobased Materials and Bioenergy 5, 442–451.
Lim, S.-K., Lee, J.-J., Jang, S.-G., Lee, S.-I., Lee, K.-H., Choi, H.J., Chin, I.-J., 2011a. Synthetic aliphatic biodegradable poly(butylene succinate)/clay nanocomposite foams with high blowing ratio and their physical characteristics. Polymer Engineering and Science 51, 1316–1324.
Lim, S.K., Lee, S.I., Jang, S.G., Lee, K.H., Choi, H.J., Chin, I.J., 2011b. Synthetic aliphatic biodegradable poly(butylene succinate)/MWNT nanocomposite foams and their physical characteristics. Journal of Macromolecular Science, Part B. Physics 50, 1171–1184.
Lin, N., Fan, D., Chang, P.R., Yu, J., Cheng, X., Huang, J., 2011. Structure and properties of poly(butylenes succinate) filled with lignin: a case of lignosulfonate. Journal of Applied Polymer Science 121, 1717–1724.
Liu, Y., Gao, L., Zheng, S., Wang, Y., Sun, J., Kajiura, H., Li, Y., Noda, K., 2007. Debundling of single-walled carbon nanotubes by using natural polyelectrolytes. Nanotechnology 18, 365702/1–365702/6.
Mahboobeh, E., Yunus, W.M.Z.W., Hussein, Z., Ahmad, M., Ibrahim, N.A., 2010. Flexibility improvement of poly(lactic acid) by stearate-modified layered double hydroxide. Journal of Applied Polymer Science 118, 1077–1083.
Mangiacapra, P., Raimondo, M., Tammaro, L., Vittoria, V., 2007. Nanometric dispersion of a Mg/Al layered double hydroxide into a chemically modified polycaprolactone. Biomacromolecules 8, 773–779.
Mohanty, S., Nayak, S.K., 2010. Biodegradable nanocomposites of poly (butylene adipate-co-terephthalate) (PBAT) with organically modified nanoclays. International Journal of Plastic Technology 14, 192–212.
Oh, J.-M., Biswick, T.T., Choy, J.-H., 2009. Layered nanomaterials for green materials. Journal of Materials Chemistry 19, 2553–2563.
Oliviero, M., Verdolotti, L., Di Maio, E., Aurilia, M., Iannace, S., 2011. Effect of supramolecular structures on thermoplastic Zein–Lignin bionanocomposites. Journal of Agricultural and Food Chemistry 59, 10062–10070.
Pandey, J.K., Kumar, A.P., Misra, M., Mohanty, A.K., Drzal, L.T., Singh, R.P., 2005. Recent advances in biodegradable nanocomposites. Journal of Nanoscience and Nanotechnology 5, 497–526.
Paul, M.-A., Alexandre, M., Degée, P., Henrist, C., Rulmont, A., Dubois, P., 2003. New nanocomposite materials based on plasticized poly(L-lactide) and organo-modified montmorillonite: thermal and morphological study. Polymer 44, 443–450.
Raquez, J.-M., Nabar, Y., Narayan, R., Dubois, P., 2011. Preparation and characterization of maleated thermoplastic starch-based nanocomposites. Journal of Applied Polymer Science 122, 639–647.
Ray, S.S., Bousmina, M., 2006. The relations between structure and mechanical properties of poly(butylene succinate-co-adipate)/montmorillonite nanocomposites. Journal of Polymer Engineering 26, 885–901.
Ray, S.S., Okamoto, K., Okamoto, M., 2003. Structure properties relationship in biodegradable poly(butylene succinate)/layered silicate nanocomposites. Macromolecules 36, 2355–2367.
Schmidt, B., Katiyar, V., Plackett, D., Larsen, E.H., Gerds, N., Koch, C.B., Petersen, J.H., 2011. Migration of nanosized layered double hydroxide platelets from polylactide nanocomposite films. Food Additives & Contaminants. Part A, Chemistry, Analysis, Control, Exposure & Risk Assessment 28, 956–966.
Siegenthales, K.O., Künkel, A., Skupin, G., Yamamoto, M., 2012. Ecoflex® and Ecovio®: biodegradable, performance-enabling plastics. In: Rieger, B., Künkel, Coates, G.W. (Eds.), Synthetic biodegradable polymers. Advances in Polymer Science. 0065-3195, 245. Springer-Verlag, Berlin Heidelberg.
Sorrentino, A., Gorrasi, G., Tortora, M.R., Vittoria, R., Costantino, U., Marmottini, F., Padella, F., 2005. Incorporation of Mg–Al hydrotalcite into a biodegradable poly(ε-caprolactone) by high energy ball milling. Polymer 46, 1601–1608.
Swanson, C.H., Stimpfling, T., Troutier-Thuilliez, A.L., Hintze-Bruening, H., Leroux, F., 2012. LDH platelets exfoliation into a water-based polyester. Journal of Applied Polymer Science. http://dx.doi.org/10.1002/APP38483.
Tsuji, H., Horikawa, G., 2007. Porous biodegradable polyester blends of poly(L-lactic acid) and poly(-caprolactone): physical properties, morphology, and biodegradation. Polymer International 56, 258–266.
Utracki, L.A., Sepehr, M., Boccaleri, E., 2007. Synthetic, layered nanoparticles for polymeric nanocomposites (PNCs). Polymers for Advanced Technologies 18, 1–37.
Wang, D.-Y., Leuteritz, A., Wang, Y.-Z., Wagenknecht, U., Heinrich, G., 2010. Preparation and burning behaviors of flame retarding biodegradable poly(lactic acid) nanocomposite based on zinc aluminum layered double hydroxide. Polymer Degradation and Stability 95, 2474–2480.
Yang, F., Qiu, Z., 2011. Preparation, crystallization, and properties of biodegradable poly(butylene adipate-co-terephthalate)/organomodified montmorillonite nanocomposites. Journal of Applied Polymer Science 119, 1426–1434.
Zhou, Q., Verney, V., Commereuc, S., Chin, I.-J., Leroux, F., 2010. Strong interfacial attrition developed by oleate/layered double hydroxide nanoplatelets dispersed into poly(butylene succinate). Journal of Colloid and Interface Science 349, 127–133.